Noname manuscript No.
(will be inserted by the editor)

Numerical schemes for the optimal input flow of a supply-chain

Ciro D'Apice · Rosanna Manzo · Benedetto Piccoli

arXiv:1208.4824v1 [math.NA] 23 Aug 2012

Received: date / Accepted: date

Abstract An innovative numerical technique is presented to adjust the inflow to a supply chain in order to achieve a desired outflow, reducing the costs of inventory, or the goods timing in warehouses.
The supply chain is modelled by a conservation law for the density of processed parts coupled to an ODE for the queue buffer occupancy. The control problem is stated as the minimization of a cost functional J measuring the queue size and the quadratic difference between the outflow and the expected one. The main novelty is the extensive use of generalized tangent vectors to a piecewise constant control, which represent time shifts of discontinuity points.
Such method allows convergence results and error estimates for an Upwind-Euler steepest descent algorithm, which is also tested by numerical simulations.

Keywords Supply chains · ODE-PDE models · Optimal control · Upwind-Euler scheme · Tangent vectors

C. D'Apice
Department of Electronic and Computer Engineering, University of Salerno, Fisciano, Salerno, Italy
Tel.: +39-089-962098
Fax: +39-089-964218
E-mail: cdapice@unisa.it

R. Manzo
Department of Electronic and Computer Engineering, University of Salerno, Fisciano, Salerno, Italy
Tel.: +39-089-964262
Fax: +39-089-964218
E-mail: rmanzo@unisa.it

B. Piccoli
Department of Mathematical Sciences, Rutgers University, Camden, NJ, US
Tel.: +1-856-2256356
Fax: +1-856-225
E-mail: piccoli@camden.rutgers.edu

Mathematics Subject Classification (2000) 35L65 · 90B30 · 76N25 · 65M08

1 Introduction

The mathematical modeling of industrial production, as well as the development of techniques for simulation and optimization purposes, is of great interest in order to reduce unwanted phenomena (bottlenecks, dead times at queues, and so on). Depending on the scale, one can distinguish different modelling approaches, for instance discrete (Discrete Event Simulations, [14]) or continuous (Differential Equations, [1,2,3,21,22]). The latter class includes models based on partial differential equations ([8,11,12,16]). For a recent review see [10].

In this paper, we focus the attention on the continuous model for supply chains proposed by Göttlich, Herty and Klar in [16], briefly GHK model. A supply chain consists of processors with constant processing rate and a queue in front of each processor. The dynamics of parts on a processor is described by a conservation law, while the evolution of the queue buffer occupancy is given by an ordinary differential equation. The latter is simply determined by the difference of fluxes between the preceding and following processors. The complete model consists of a coupled PDE-ODE system.
Various optimal problems, corresponding to different types of controls, have been analysed for the GHK model (see [13,17,18,19,23]). Typically one may consider the input flow to the whole supply chain as a control as well as production rates and distribution coefficients in case of supply networks. These papers provide a number of results and, in particular, numerical algorithms to find the optimal control. In [23] two discretization techniques are compared: one consisting in first writing the adjoint system and then discretizing, while the second consists in inverting the order, that is first discretizing and then writing the adjoint system. All these methods compete with Discrete Events ones for numerical accuracy and computational times, see also [10].

In this paper we focus on the optimal control problem, where the control is given by the input flow to the supply chain and the cost functional J is the sum of time-integral of queues and quadratic distance from a preassigned desired outflow. In [13], piecewise constant controls are considered together with generalized tangent vectors, which represent time shifts of discontinuities of the control. The technique of such generalized tangent vectors was extensively used for conservation laws, see [7], and for the case of network models, see [15, 20]. The main result of [13] is the existence of optimal controls.

The aim of this work is to introduce an innovative numerical approach, which builds up on the idea of generalized tangent vectors. Let us first explain in rough words the core idea of the approach. A good numerical method, in theory and practice, for an optimization problem is often based on a suitable choice of "perturbations". Then one can define critical points, according to the chosen perturbations, and numerical algorithms stemming from such def-

inition.
We base our method on perturbations of piecewise constant controls, obtained by time shifting the discontinuity points. The advantage of this method is twofold: on one side generalized tangent vectors are well suited for Wave Front Tracking (briefly WFT, see [6,15]) algorithms, which allow theoretical estimates on convergence rate. On the other side, generalized tangent vectors have a particularly simple evolution in time, which can be conveniently adapted to easily implementable methods as Upwind-Euler (briefly UE, see [9]). Moreover, in [9] convergence of the UE algorithm was proved by measuring the distance with WFT solutions by generalized tangent vectors.
The discretization of the evolution of generalized tangent vectors allows the numerical computation of the cost functional gradient. This can be combined with classical steepest descent or more advanced Newton methods for the optimization procedure by iterations.
Now, the results which complete the picture is the following. To estimate the gradient of the cost functional we can use alternatively WFT or UE algorithms for the evolution of generalized tangent vectors. Even more, we can measure the distance among the two, by again using suitably defined tangent vectors. This, in turn, allows to provide convergence results and error estimates.
Finally simulations are performed to show results for the proposed numerical algorithm in some case studies.

The outline of the paper is the following. In Section 2, we describe the GHK model and introduce the optimal control problem. The WFT algorithm to construct approximate solutions to the model is illustrated in Section 3, together with the definition and evolution of generalized tangent vectors. Then Section 4 describes the UE numerical algorithm for solutions to the coupled ODE-PDE system and also the numerics for generalized tangent vectors and cost functional derivative. Convergence results and rates for our method are then given in Section 5. Finally some numerical tests are discussed in Section 6.

2 An optimal control problem for supply chains

A supply chain consists of consecutive suppliers. Each supplier is composed of a processor for parts assembling and construction and a queue, located in front of the processor, for unprocessed parts. Formally we have the following definition.

Definition 1 A supply chain consists of a finite sequence of consecutive processors I_j, $j \in \mathcal{J} = \{1, \dots, P\}$ and queues in front of each processor, except the first. Thus the supply chain is given by a graph $G = (V, \mathcal{J})$ with arcs representing processors and vertices, in $\mathcal{V} = \{1, \dots, P-1\}$, representing queues. Each processor is parametrized by a bounded closed interval $I_j = [a_j, b_j]$, with $b_{j-1} = a_j, j = 2, ..., P$.

The maximal processing rate μ_j, and the processing velocity, given by $v_j = L_j/T_j$ with T_j and $L_j = b_j - a_j$ the processing time and the length of

the j-th processor, are constant parameters for each arc. The dynamics of the j-th processor is given by a conservation law

$$\partial_t \rho_j(x,t) + \partial_x \min\{\mu_j, v_j \rho_j(x,t)\} = 0, \quad \forall x \in [a_j, b_j], t \in \mathbb{R}^+, \tag{1}$$

$$\rho_j(x,0) = \rho_{j,0}(x), \quad \rho_j(a_j,t) = \frac{f_{j,inc}(t)}{v_j},$$

where $\rho_j \in [0, \rho_j^{max}]$ is the unknown function, representing the density of parts, while the initial datum $\rho_{j,0}$ and the inflow $f_{j,inc}(t)$ are to be assigned. An input profile $u(t)$ on the left boundary $\{(a_1,t) : t \in \mathbb{R}\}$ is given for the first arc of the supply chain. Each queue buffer occupancy is modelled as a time-dependent function $t \to q_j(t)$, satisfying the following equation:

$$\dot{q}_j(t) = f_{j-1}(\rho_{j-1}(b_{j-1},t)) - f_{j,inc}, \quad j = 2, ..., P, \tag{2}$$

where the first term is defined by the trace of ρ_{j-1} (which is assumed to be of bounded variation on the x variable), while the second is defined by:

$$f_{j,inc} = \begin{cases} \min\{f_{j-1}(\rho_{j-1}(b_{j-1},t)), \mu_j\} & \text{if } q_j(t) = 0, \\ \mu_j & \text{if } q_j(t) > 0. \end{cases} \tag{3}$$

This allows for the following interpretation: If the outgoing buffer is empty, we process as many parts as possible but at most μ_j. If the buffering queue contains parts, then we process at the maximal possible rate, namely again μ_j. Finally, the supply chain model is a coupled system of partial and ordinary differential equations given by

$$\begin{cases} \partial_t \rho_j(x,t) + \partial_x \min\{\mu_j, v_j \rho_j(x,t)\} = 0 & j = 1, ..., P, \\ \dot{q}_j(t) = f_{j-1}(\rho_{j-1}(b_{j-1},t)) - f_{j,inc}(t) & j = 2, ..., P, \\ q_j(0) = q_{j,0} & j = 2, ..., P, \\ \rho_j(x,0) = \rho_{j,0}(x) & j = 1, ..., P, \\ \rho_j(a_j,t) = \frac{f_{j,inc}(t)}{v_j} & j = 1, ..., P, \\ f_{1,inc}(t) = u(t) \end{cases} \tag{4}$$

where $f_{j,inc}$ is given by (3), for $j = 2, ..., P$.

Fixed a time horizon $[0,T]$, define the cost functional:

$$\begin{aligned} J(u) &= \sum_{j=2}^{P} \int_0^T \alpha_1(t)\, q_j(t) dt + \int_0^T \alpha_2(t)\, \left[v_P \cdot \rho_P(b_P,t)) - \psi(t)\right]^2 dt \\ &\doteq J_1(u) + J_2(u), \end{aligned} \tag{5}$$

where $\alpha_1 \in L^1\big((0,T),[0,+\infty)\big)$, $\alpha_2 \in \mathrm{Lip}\big((0,T),[0,+\infty)\big)$ (the space of Lipschitz continuous functions) are weight functions, (ρ_j, q_j) is the solution to (4) for the control u, $v_P \cdot \rho_P(b_P,t))$ represents the outflow of the supply chain (assuming the density level is below μ_P), while $\psi(t) \in \mathrm{Lip}\big((0,T),[0,+\infty)\big)$ is

a pre-assigned desired outflow. Given $C > 0$, we consider the minimization problem

$$\min_{u \in \mathcal{U}_C} J(u) \tag{6}$$

where $\mathcal{U}_C = \{u : [0,T] \to [0,\mu_1]\,;\, u \text{ measurable, } T.V.(u) \leq C\}$ (with $T.V.$ indicating the total variation). In other words, we want to minimize the queues length and the distance between the exiting flow and the pre-assigned flow $\psi(t)$, using the supply chain input u as control.

In [13], the existence of an optimal control was proved for a general problem, which includes the case (4)-(6):

Theorem 1 *(see [13]) Consider the optimal control problem (4), (6). If J is lower semicontinuous for the L^1 norm, then there exists an optimal control.*

Our aim is now to provide a new approach to solve (4)-(6) numerically. The key idea is to focus on piecewise constant controls and perturb the position of discontinuity points. The procedure corresponds to define (generalized) tangent vectors to u (in the spirit of [7]). We can then take advantage of the knowledge of time evolution of such tangent vectors, developed in [20].
More precisely, we start giving the following:

Definition 2 We indicate by $\widetilde{\mathcal{U}} \subset \mathcal{U}_C$ the set of Piecewise Constant controls. For every $u \in \widetilde{\mathcal{U}}$ we indicate by $\tau_k = \tau_k(u)$, $k = 1, \ldots, \delta(u)$, the discontinuity points of u.

We are now ready to define the perturbation to a piecewise constant control:

Definition 3 Given $u \in \widetilde{\mathcal{U}}$, a tangent vector to u is a vector $\xi = (\xi_1, \ldots, \xi_{\delta(u)}) \in \mathbb{R}^{\delta(u)}$ representing shifts of discontinuities. The norm of the tangent vector is defined as:

$$\|\xi\| = \sum_{k=1}^{\delta(u)} |\xi_k| \cdot |u(\tau_k+) - u(\tau_k-)|\,.$$

Assume now for simplicity that $\tau_1 > 0$, $\tau_{\delta(u)} < T$, and set $\tau_0 = 0$, $\xi_0 = 0$, $\tau_{\delta(u)+1} = T$, $\xi_{\delta(u)+1} = 0$. Then given a tangent vector ξ to u, for every ε sufficiently small we define the infinitesimal displacement as:

$$u_\varepsilon = \sum_{k=0}^{\delta(u)} \chi_{[\tau_k+\varepsilon\xi_k, \tau_{k+1}+\varepsilon\xi_{k+1}[} u(\tau_k+), \tag{7}$$

where χ is the indicator function. In other words u_ε is obtained from u by shifting the discontinuity points of $\varepsilon\xi$ (see Figure 1).

Remark 1 The notion of tangent vector to piecewise constant function was introduced in [5] and used in [7] to prove uniqueness and continuous dependence of solutions to systems of conservation laws.

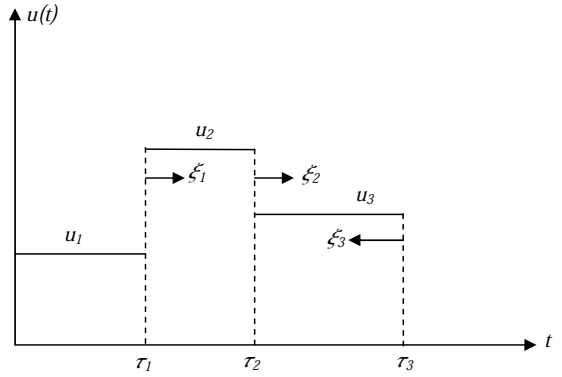


Fig. 1 Shifting of the discontinuity points of the control u.

More precisely, one defines a distance of Finsler type among piecewise constant functions by considering paths which admit tangent vectors. Then, by density and using the usual L^1 metric one can extend the metric to the whole L^1. Finally one may study the evolution of tangent vectors and, in particular, estimates on their norms.
This same technique was generalized to flows on networks, see [15], and to the GHK supply chain model, see [20].

In next sections we are going to define numerical schemes for the solution of (4) and for the evolution of tangent vectors. The latter, in turn, will provide the information for the computation of numerical gradient of the cost functional J.
The evolution of tangent vectors is particularly clear for the theoretical numerical scheme given by the WFT algorithm. This was used in [9] to prove convergence of an Upwind-Euler scheme and in [13] to obtain the existence of an optimal control for (4)-(6). We thus recall briefly the WFT algorithm and the evolution of tangent vectors along approximate solutions constructed via the WFT algorithm.

3 The Wave Front Tracking algorithm

In this section we explain how to construct piecewise constant approximate solutions to (4) by WFT method, see [6] for details.

Given a discretization parameter σ and initial conditions $\rho_{j,0}$ in BV, the space of bounded variation functions, a WFT approximate solution is constructed by a procedure sketched by the following steps:

– Approximate the initial datum by a piecewise constant function (with discretization parameter σ) and solve the Riemann Problems (RPs) corresponding to discontinuities of the approximation. In RPs solutions approximate rarefactions by rarefaction shocks of size σ;

- Use the piecewise constant solution obtained piecing together the solutions to RPs up to the first time of interaction of two shocks;
- Then solve the new RP created by interaction of waves and prolong the solution up to next interaction time, and so on.

To ensure the feasibility of such construction and the convergence of WFT approximate solutions to a weak solution as $\sigma \to 0$, it is enough to control the number of waves and interactions and the BV norm. This is easily done in scalar case since both the number of waves and the BV norm are decreasing in time (see [6] for details).
For our system, we need also to approximate the queue evolution. For this we compute the exact solutions to (2) (see [20] for BV estimates for the complete PDE-ODE model (4)).

Notice that, as soon as a boundary datum will achieve a value below μ_j, then in finite time all values above μ_j will disappear from the j-th processor, see also [20]. Therefore, for simplicity, we will assume

(H1) $\rho_{j,0}(x) \leq \mu_j$ for all $j \in \mathcal{J}$.

Then the same inequality will be satisfied for all times. In this case solutions to RPs are particularly simple, indeed the conservation law is linear, thus given some Riemann data (ρ_-, ρ_+) on the j-th processor, the solution is always given by a shock travelling with velocity v_j.

3.1 Tangent vectors evolution

The infinitesimal displacement of each discontinuity of the control u produces changes in the whole supply chain, whose effects are visible both on processors and on queues. In fact, every shift ξ generates shifts on the densities and shifts on the queues, which spread along the whole supply chain.
Since the control u is piecewise constant, the solution (ρ_j, q_j) to (4) is such that ρ_j is piecewise constant and q_j is piecewise linear. A tangent vector to the solution (ρ_j, q_j) is given by:

$$({}^{\beta}\xi_j, \eta_j),$$

where β runs over the set of discontinuities of ρ_j, ${}^{\beta}\xi_j$ are the shifts of the discontinuities, while η_j is the shift of the queue buffer occupancy q_j. The norm of a tangent vector is given by:

$$\|({}^{\beta}\xi_j, \eta_j)\| = \sum_{\beta} |{}^{\beta}\xi_j||\Delta^{\beta}\rho_j| + \sum_j |\eta_j|, \tag{8}$$

where $\Delta^{\beta}\rho_j = {}^{\beta}\rho_l^j - {}^{\beta}\rho_r^j$ is the jump in ρ of the discontinuity β (where ${}^{\beta}\rho_l^j$, respectively ${}^{\beta}\rho_r^j$, is the value on the left, respectively right, of the discontinuity β).
Notice that this is compatible with the definition of norm of tangent vector

to a control. Because of assumption (H1), we have no wave interaction inside the processors. Therefore, densities and queues shifts remain constant for almost all times and change only at those times at which one of the following interactions occurs:

a) interaction of a density wave with a queue;
b) emptying of the queue.

We now provide formulas for such changes. Assume a wave with shift ${}^{\beta}\xi_{j-1}$ interact with the j-th queue and let $\bar{t}$ be the interaction time. We use the letters $+$ and $-$ to indicate quantities before and after $\bar{t}$, respectively. So, we indicate with ρ_j^- and ρ_j^+ the densities on the processor I_j before and after an interaction occurs and similarly for I_{j-1}. Also we use ${}^{\beta}\xi_j$ to denote the shift on the processor I_j and with ${}^{\beta}\eta_j^-$ and ${}^{\beta}\eta_j^+$ the shifts on the queue q_j, respectively before and after the interaction. Consider the case **a)** and distinguish two subcases:

a.1) $q_j(\bar{t}) = 0$;
a.2) $q_j(\bar{t}) > 0$.

In case **a.1)** we have to further distinguish two subcases:

a.1.1) if $v_{j-1}\rho_{j-1}^+ < v_{j-1}\rho_{j-1}^- < \mu_j$, then ${}^{\beta}\xi_j = \frac{v_j}{v_{j-1}}{}^{\beta}\xi_{j-1}$ and ${}^{\beta}\eta_j^- = 0 = {}^{\beta}\eta_j^+$;

a.1.2) if $v_{j-1}\rho_{j-1}^+ > \mu_j$, then ${}^{\beta}\xi_j = \frac{v_j}{v_{j-1}}{}^{\beta}\xi_{j-1}$ and ${}^{\beta}\eta_j^+ = {}^{\beta}\xi_{j-1}\frac{(v_{j-1}\rho_{j-1}^+ - \mu_j)}{v_{j-1}} + {}^{\beta}\eta_j^-$.

In case **a.2)** we have: ${}^{\beta}\xi_j = 0$, ${}^{\beta}\eta_j^+ = {}^{\beta}\xi_{j-1}(\rho_{j-1}^- - \rho_{j-1}^+) + {}^{\beta}\eta_j^-$.
Finally in case **b)** we get: ${}^{\beta}\eta_j^+ = 0$, ${}^{\beta}\xi_{j-1} = 0$ and ${}^{\beta}\xi_j = -\frac{v_j\,{}^{\beta}\eta_j^-}{(v_{j-1}\rho_{j-1}^- - \mu_j)}$.

Using the above notations, indicate by ${}^{\beta}\xi_P$ the shift to a generic discontinuity of ρ_P and by ${}^{\beta}\rho_P^+$, respectively ${}^{\beta}\rho_P^-$, the value of ρ_P on the right, respectively left, of the discontinuity. The following holds:

Proposition 1 *Consider a control $u \in \widetilde{\mathcal{U}}$ and a tangent vector $\xi \in \mathbb{R}^{\delta(u)}$ to u. The gradient of the cost functional J with respect to ξ is given by:*

$$\nabla_\xi J(u) = \sum_j \int_0^T \alpha_1(t)\eta_j(t)dt + \sum_\beta \alpha_2(t^\beta)\, v_P \left({}^{\beta}\rho_P^+ + {}^{\beta}\rho_P^- - 2\psi(t^\beta)\right) {}^{\beta}\xi_P\, \Delta({}^{\beta}\rho_P)$$
$$\doteq Y_1^{WFT} + Y_2^{WFT}, \tag{9}$$

where $\Delta({}^{\beta}\rho_P) = {}^{\beta}\rho_P^+ - {}^{\beta}\rho_P^-$ and t^β is the interaction time of the discontinuity indexed by β with b_P, the right extreme of the supply chain.

Proof We have $\nabla_\xi J(u) = \lim_{\varepsilon\to 0}\frac{J(u_\varepsilon)-J(u)}{\varepsilon|\xi|}$. By definition of the functional J, the infinitesimal change Y_1^{WFT} in J_1 due to the infinitesimal displacement $\varepsilon\xi$ of the control u is

$$Y_1^{WFT} = \varepsilon \sum_j \int_0^t \alpha_1(t^\beta)\eta_j(t)dt, \tag{10}$$

while the infinitesimal change Y_2^{WFT} in J_2 is

$$Y_2^{WFT} = \varepsilon \sum_{\beta} \alpha_2(t^\beta)\, v_P \left[\left({}^\beta\rho_P^+\right)^2 - \left({}^\beta\rho_P^-\right)^2 - 2\psi(t^\beta)\left({}^\beta\rho_P^+ - {}^\beta\rho_P^-\right)\right] {}^\beta\xi_P, \tag{11}$$

thus we conclude.

4 Steepest descent for the Upwind-Euler scheme

In this section we introduce first an Upwind-Euler scheme for the system (4) and then a numerical scheme for the evolution of the tangent vectors to a solution to the PDE-ODE model. From the latter we will be able to compute numerically the derivative of the cost functional with respect to the discontinuities of the input flow. This, in turn, will be used in steepest descent methods to find the optimal control.
For a general introduction to numerical schemes for conservation laws we refer to [24], while for optimization algorithms to [4].

For simplicity we assume:

(H2) The lengths L_j are rationally dependent.

Assumption (H2) allows us to use a unique space mesh for all processors I_j, $j = 1, \dots, P$. Indeed there exists Δ so that all L_j are multiple of Δ and we will always use time and space meshes dividing Δ.

Remark 2 It is possible to choose different space and/or time grid meshes for different processors. This is necessary in the general case in which the lengths of arcs have not rational ratios. Details can be found in [9].

In next section we report briefly the Upwind-Euler method, analysed in [9] to construct numerical solutions to the supply chain model (4).

4.1 Upwind-Euler scheme for supply chains

Given a space mesh Δx, for each processor I_j, we set $\Delta t_j = \Delta x / v_j$ and define a numerical grid of $[0, L_j] \times [0, T]$ by:

- $(x_i, t^n)_j = (i\Delta x,\ n\Delta t_j)$, $i = 0, ..., N_j$, $n = 0, ..., M_j$ are the grid points;
- ${}^j\rho_i^n$ is the value taken by the approximated density at the point $(x_i, t^n)_j$;
- q_j^n is the value taken by the approximate queue buffer occupancy at time t^n.

The Upwind method reads:

$${}^j\rho_i^{n+1} = {}^j\rho_i^n - \frac{\Delta t_j}{\Delta x} v_j \left({}^j\rho_i^n - {}^j\rho_{i-1}^n \right) = {}^j\rho_{i-1}^n, \tag{12}$$

where $j \in \mathcal{J}$, $i = 0, ..., N_j$ and $n = 0, ..., M_j$. Notice that the CFL condition is given by $\Delta t_j \leq \frac{\Delta x}{v_j}$, and thus holds true. The explicit Euler method is given by:

$$q_j^{n+1} = q_j^n + \Delta t_j \left(f_{j-1}^n - f_{j,inc}^n \right), \ j \in \mathcal{J} \setminus \{1\}, \ n = 0, ..., M_j, \tag{13}$$

where f_{j-1}^n needs to be defined and

$$f_{j,inc}^n = \begin{cases} \min\left\{ f_{j-1}({}^{j-1}\rho_{N_{j-1}}^n), \mu_j \right\} & q_j^n(t) = 0, \\ \mu_j & q_j^n(t) > 0. \end{cases} \tag{14}$$

Now, if $\Delta t_{j-1} \leq \Delta t_j$ we set:

$$f_{j-1}^n = \sum_{l=1}^{M(n)-m(n)-1} \Delta t_{j-1} f_{j-1}({}^{j-1}\rho_{N_{j-1}}^{m(n)+l}) = \sum_{l=1}^{\gamma} \Delta t_{j-1} f_{j-1}({}^{j-1}\rho_{N_{j-1}}^{\gamma n+l}), \tag{15}$$

where $m(n)$ and $M(n)$ are defined as:

$$m(n) = \sup \{ m : m\Delta t_{j-1} \leq n\Delta t_j \},$$

$$M(n) = \inf \{ M : M\Delta t_{j-1} \geq (n+1)\Delta t_j \}.$$

Otherwise, that is if $\Delta t_{j-1} > \Delta t_j$, we set:

$$f_{j-1}^n = f_{j-1}\left({}^{j-1}\rho_{N_{j-1}}^{\lfloor \frac{n\Delta t_j}{\Delta t_{j-1}} \rfloor} \right), \tag{16}$$

where $\lfloor \cdot \rfloor$ indicates the floor function. Boundary data are treated using ghost cells and the expression of inflows given by (14). The convergence of the scheme has been proved in [9] using a comparison with WFT approximate solutions.

4.2 Numerics for tangent vectors and cost functional

We first completely discretize the control space via the time mesh Δt:

$$\widetilde{\mathcal{U}}_{\Delta t} = \{ u \in \widetilde{\mathcal{U}} : \tau_k(u) = n(u,k)\,\Delta t, \ n(k,u) \in \mathbb{N}, \ k = 1, \ldots, \delta(u) \}. \tag{17}$$

Now for every $u \in \widetilde{\mathcal{U}}_{\Delta t}$ we consider shifts ξ so that the obtained time-shifted control is still in $\widetilde{\mathcal{U}}_{\Delta t}$. Then every ξ_k is necessarily a multiple of Δt. Hence from now on we will restrict to the case:

$$\xi_k = \pm \Delta t, \quad k = 1, \ldots, \delta(u). \tag{18}$$

For a generic processor I_j and a discontinuity point τ_k of the control, we denote by ${}^{k,j}\xi_i^n$ and ${}^{k,j}\eta^n$ the approximations of ${}^k\xi_j(x_i, t^n)$, and ${}^k\eta_j(t^n)$, respectively. We define such approximations by a recursive procedure explained

in the following.
We initialize the tangent vector approximations by setting:

$$\begin{aligned} {}^{k,j}\xi_i^n &= 0, \quad \text{for } n = 1, \dots, n(k-1,u),\ j = 1, \dots, P, \\ {}^{k,1}\xi_1^{n(k,u)} &= v_1\,(\pm\Delta t), \\ {}^{k,j}\eta^0 &= 0, \quad j = 1, \dots, P. \end{aligned} \tag{19}$$

The definition of ${}^{k,1}\xi_1^{n(k,u)}$ reflects the fact that the shift ξ_k provokes a shift of the wave generated on the first processor.
Now, the evolution of approximations of tangent vectors to ρ inside processors is simply given by:

$${}^{k,j}\xi_i^{n+1} \;=\; {}^{k,j}\xi_{i-1}^n.$$

On the other side, the approximation of ξ and η influence each other at interaction times with queues. More precisely, we consider the four cases described in Section 3.1 and get:

a.1.1): ${}^{k,j}\eta^{n+1} = 0,\ {}^{k,j}\xi_1^{n+1} = \frac{v_j}{v_{j-1}}\ {}^{k,j-1}\xi_{N_{j-1}}^n$;

a.1.2): ${}^{k,j}\xi_1^{n+1} = \frac{v_j}{v_{j-1}}\ {}^{k,j-1}\xi_{N_{j-1}}^n,\ {}^{k,j}\eta^{n+1} = {}^{k,j-1}\xi_{N_{j-1}}^n \frac{\left(v_{j-1}\ {}^{j-1}\rho_{N_{j-1}}^{n+1} - \mu_j\right)}{v_{j-1}} +$ ${}^{k,j}\eta^n$;

a.2): ${}^{k,j}\xi_1^{n+1} = 0,\ {}^{k,j}\eta^{n+1} = {}^{k,j-1}\xi_{N_{j-1}}^n \left({}^{j-1}\rho_{N_{j-1}}^{n+1} - {}^{j-1}\rho_{N_{j-1}}^n\right) + {}^{k,j}\eta^n$;

b): ${}^{k,j-1}\xi_{N_{j-1}}^n = 0,\ {}^{k,j}\eta^{n+1} = 0,\ {}^{k,j}\xi_1^{n+1} = -\frac{v_j\ {}^{k,j}\eta^n}{v_{j-1}\ {}^{j-1}\rho_{N_{j-1}}^n - \mu_j}$.

Notice that this is compatible with the evolution of tangent vectors along WFT approximate solutions and also the norm of approximate tangent vectors, in the sense of (8), is conserved.

Now we are ready to compute numerical approximations for $\nabla_\xi J$. We denote by ${}^{k,j}Y_1^n$, respectively ${}^kY_2^n$, the numerical approximations of the k-th component of Y_1^{WFT}, respectively Y_2^{WFT}, as defined in (9) on processor I_j at time t^n.
We initialize such approximation by setting:

$${}^{k,j}Y_1^0 = 0,\ {}^kY_2^0 = 0, \quad j = 1, \dots, P,\ k = 1, \dots, \delta(u). \tag{20}$$

Now the evolution is determined by the following simple rules. For Y_1, if $q_j^{n+1} > 0$, then we set

$${}^{k,j}Y_1^{n+1} = {}^{k,j}Y_1^n + \alpha_1(t^n)\ {}^{k,j}\eta^n \triangle t,$$

while for $q_j^{n+1} = 0$ we distinguish two subcases:

- if $q_j^n = 0$, then ${}^{k,j}Y_1^{n+1} = {}^{k,j}Y_1^n$;
- if $q_j^n > 0$, then ${}^{k,j}Y_1^{n+1} = {}^{k,j}Y_1^n + \frac{1}{2}\ \alpha_1(t^n)\,{}^{k,j}\xi_1^{n+1}\ {}^{k,j}\eta^n$.

For Y_2 we set:

$${}^kY_2^{n+1} = {}^kY_2^n + \alpha_2(t)\,v_P \left(\left({}^P\rho_{N_P}^n - \psi(t^n)\right)^2 - \left({}^P\rho_{N_P}^{n+1} - \psi(t^n)\right)^2\right)\ {}^{k,P}\xi_{N_P}^n.$$

A steepest descent algorithm, denoting whit ϑ the iteration step, is defined by setting

$$\tau_k^{\vartheta+1} = \tau_k^{\vartheta} + \lfloor \frac{h_\theta \left(\sum_j \sum_n {}^{k,j}Y_1^n + \sum_n {}^{k}Y_2^n \right)}{\Delta t} \rfloor \Delta t,$$

where h_θ is a coefficient to be suitably chosen. More precisely the parameter h_θ may be chosen to solve an optimization problem to get specific schemes, see [4].

5 Convergence and error estimates

In this section we will provide convergence results and error estimates for the Upwind-Euler steepest descent scheme illustrated in Section 4. We will make use of two natural parameters $\nu \in \mathbb{N}$ and $\theta \in \mathbb{N}$, the first referring to the Upwind-Euler (and WFT) discretization, while the second indicating the iterative step of the steepest descent algorithm.

We fix an initial space mesh Δx (of which Δ is a multiple, see (H2)) and define $\Delta x_\nu = 2^{-\nu}\Delta x$. On each processor I_j the time mesh is set as:

$$\Delta t_{j,\nu} = \frac{\Delta x_\nu}{v_j},$$

thus granting the CFL condition. Obviously $\Delta t_{j,\nu} \to 0$, $\Delta x_\nu \to 0$ as ν tends to $+\infty$.

The initial datum $\rho_{j,0}$ (see (4)) is sampled in the following way:

$${}^{\nu,j}\rho_i^0 = \rho_{j,0}\big((a_j + i\, 2^{-\nu}\Delta x)\ +\big). \tag{21}$$

A control function $u_{\nu,\theta}$ will be defined by the iteration step of the steepest descent algorithm starting from a fixed $u_{\nu,0} \in \widetilde{\mathcal{U}}_{\Delta t_{1,\nu}}$. We will denote the discontinuity points of $u_{\nu,\theta}$ by $\tau_k^{\nu,\theta}$, for $k = 1, \ldots, \delta(u_{\nu,\theta})$.
Notice approximations can be constructed in such a way that $\delta(u_{\nu,\theta}) \to +\infty$ as $\nu \to +\infty$.

For simplicity ${}^{\nu,\theta}(\rho, q)^{UE}$ will denote the numerical solution generated by the Upwind-Euler scheme, i.e. the collection ${}^{\nu,\theta}({}^{j}\rho_i^n, q_j^n)$ for $j = 1, \ldots, P$, $n = 1, \ldots, M_j^\nu$, $i = 1, \ldots, N_j^\nu$. Similarly ${}^{\nu,\theta}(\xi, \eta)^{UE}$ will denote the numerical tangent vectors computed as in Section 4, i.e. the collection ${}^{\nu,\theta}({}^{k,j}\xi_i^n, {}^{k,j}\eta^n)$ for $j = 1, \ldots, P$, $n = 1, \ldots, M_j^\nu$, $i = 1, \ldots, N_j^\nu$, $k = 1, \ldots, \delta(u_{\nu,\theta})$.
We will also use the symbols ${}^{\nu,\theta}(\rho, q)^{WFT}$, respectively ${}^{\nu,\theta}(\xi, \eta)^{WFT}$, to indicate the solutions, respectively tangent vectors, produced by the Wave Front Tracking algorithm.

Now define:

$$\pi_{PC}\left({}^{\nu,j}\rho^n\right) = \sum_{i=0}^{L_j/2^{-\nu}\Delta x_j - 1} {}^{\nu,j}\rho_i^n\, \chi_{[a_j + i\, 2^{-\nu}\Delta x_j,\, a_j + (i+1)2^{-\nu}\Delta x_j[}, \tag{22}$$

and

$$\pi_{PL}\left({}^{\nu}q_j\right)(t) = {}^{\nu}q_j^n + (t - n\Delta t_{j,\nu})({}^{\nu}q_j^{n+1} - {}^{\nu}q_j^n) \qquad \text{for } t \in [n\Delta t_{j,\nu}, (n+1)\Delta t_{j,\nu}[.$$

Notice that π_{PC}, respectively π_{PL}, are operators taking values on the space of piecewise continuous, respectively piecewise linear, functions.

In [9] it was proved the following:

Theorem 2 *Assume that (H1), (H2), (21) hold true and that $\rho_{j,0}$ are of bounded variation. Then ${}^{\nu,\theta}(\rho, q)^{WFT}$ is approximated by ${}^{\nu,\theta}(\pi_{PC}(\rho), \pi_{PL}(q))^{UE}$, more precisely:*

$$\begin{aligned} &\|{}^{\nu,\theta}\rho^{WFT}(t) - {}^{\nu,\theta}(\pi_{PC}(\rho^{UE}))(t)\|_{L^1} + \|{}^{\nu,\theta}q^{WFT}(t) - {}^{\nu,\theta}(\pi_{PL}(q^{UE}))(t)\| \\ &\leq 2^{-\nu}\ K\big(T.V.(\rho_{j,0}), \mu_j\big), \end{aligned} \tag{23}$$

where K is a suitable constant depending only on the total variation of $\rho_{j,0}$ and the values μ_j, $j = 1, \dots, P$.
Moreover ${}^{\nu,\theta}(\pi_{PC}(\rho), \pi_{PL}(q))^{UE}$ converges to a solution of (4) with a convergence rate as in (23).

The main idea behind Theorem 2 is to use tangent vectors to estimate the distance among WFT and UE approximate solutions. In the same fashion we are now going to estimate the distance among tangent vectors computed via WFT and UE schemes.

In each processor I_j, the WFT wave shifts ${}^{\beta}\xi_j(t^n)$ are approximated by the UE shifts ${}^{k,j}\xi_i^n$ in the following sense. Each shift ${}^{\beta}\xi_j(t^n)$ corresponds to one or more non vanishing values of ${}^{k,j}\xi_i^n$, whose position is possibly shifted by some amount. By splitting the shift ${}^{\beta}\xi_j(t^n)$ in one or more pieces, whose sum is equal to ${}^{\beta}\xi_j(t^n)$, we can define the difference with the UE generated shifts by tangent vectors ${}^{\beta}\zeta_j(t^n)$, which represent the space distance among the location of the discontinuity β of ρ_j at time t^n and the location of the non vanishing values of ${}^{k,j}\xi_i^n$, i.e. $a_j + i\,\Delta x_\nu$.
For instance in the WFT algorithm a shift ξ_k, of the time discontinuity τ_k, gives rise to a shift $\xi = v_1\xi_k$ on processor I_1 at time τ_k of the wave generated by the discontinuity τ_k. Similarly the UE algorithm will generate a non vanishing value ${}^{k,1}\xi_1^{n(k,u)} = v_1\xi_k$. Therefore, we have $\zeta_1(\tau_k) = \zeta_1(n(k,u)\Delta t_{1,\nu}) = 0$, indeed the WFT and UE shifts coincide.
Analougsly we define the tangent vectors ι_j to the queue shifts η_j generated by WFT to recover those generated by UE.
We define the norm of the tangent vectors (ζ, ι) in the following way:

$$\|(\zeta, \iota)\| = \sum_j \sum_\beta |{}^{\beta}\zeta_j|\,|{}^{\beta}\xi_j|\,|\Delta\rho_j^{\beta}| + \sum_j |\iota_j|\,|\eta_j|. \tag{24}$$

In particular we have:

$$\|(\zeta, \iota)(0)\| = 0. \tag{25}$$

Such tangent vectors (ζ, ι) evolve using the same rules of (ξ, η) for the Wave Front Tracking algorithm, see Section 3.1. In particular their norm may

increase because of interactions with queues. Moreover, the norm may also increase because of errors produced by the use of different time meshes among different processors, see formula (15) and (16). Summarizing, to estimate the increase in (ζ, ι) norm we have to consider:

i) approximation errors occurring at interaction of waves with queues and at time in which a queue empties;
ii) the approximation errors due to different time discretizations $\Delta t_{j,\nu}$.

Let us start by considering the case i) assuming there is no error approximation because of different time meshes. Since the evolution of (ζ, ι) follows the same rules as those of (ξ, η) for WFT, we can use the same estimates established in [9]. Referring to formulas (29), (30) and (31) of [9], and using the symbols $\pm$ to indicate quantities before and after the interaction, we get:

$$\|(\zeta,\iota)_+\| \leq \left(\max\left\{\frac{v_j}{v_{j-1}}, 1\right\}\right) \|(\zeta,\iota)_-\| + v_j\,|\eta_j^-|\,\Delta t_{j,\nu}\,|\Delta\rho_j|, \tag{26}$$

where j is the queue involved in the interaction and $\Delta\rho_j$ is the jump in ρ of the wave exiting to processor I_j. More precisely, the first term on the right of (26) is sufficient for the case of interaction of a wave with a queue, see also (29) and (30) of [9]. In case of emptying of the queue q_j, the first term takes into account the evolution of (η, ι), as described in Section 3.1. The second term takes into account the additional shifts, provoked by the fact that the WFT produces a wave in I_j at a time which may be not a multiple of $\Delta t_{j,\nu}$ (as it happens for all waves of the UE algorithm), see also formula (31) of [9].

Regarding ii), we refer to formulas (15) and (16). In case of $\Delta t_{j-1,\nu} > \Delta t_{j,\nu}$, then no additional error occurs. Otherwise, the error is estimated by:

$$\|(\zeta,\iota)_+\| \leq \|(\zeta,\iota)_-\| + v_j\,\Delta t_{j-1,\nu}\,|\xi_{j-1}|\,|\Delta\rho_{j-1}|,$$

where ξ_{j-1} is the shift of the interacting wave and $\Delta\rho_{j-1}$ is the jump in ρ of the interacting wave.

Recalling (25), from the above estimates we get the following:

$$\sup_{t\in[0,T]} \|(\zeta,\iota)(t)\| \leq \prod_{j=2}^{P} \max\left\{\frac{v_j}{v_{j-1}}, 1\right\}$$

$$\cdot \max_j v_j \Delta t_{j,\nu} \cdot \sup_{t\in[0,T]} \|\,{}^{\nu,\theta}(\xi,\eta)^{WFT}(t)\| \cdot \sup_{t\in[0,T]} T.V.({}^{\nu,\theta}\rho^{WFT}(t)). \tag{27}$$

Now in [20] it was proved (Lemma 2.7) that the norm of tangent vectors are decreasing along WFT solutions. Moreover, the tangent vectors for the WFT solutions satisfy the same initial estimate as (19), thus we get:

$$\sup_{t\in[0,T]} \|\,{}^{\nu,\theta}(\xi,\eta)^{WFT}(t)\| \leq \|\,{}^{\nu,\theta}(\xi,\eta)^{WFT}(0)\| = v_1\,\Delta t_{1,\nu} = \Delta x_\nu = 2^{-\nu}\Delta x. \tag{28}$$

From (2.10a) of [20] and (21), we get:

$$\sup_{t\in[0,T]} T.V.({}^{\nu,\theta}\rho^{WFT}(t)) \le T.V.({}^{\nu,\theta}\rho^{WFT}(0)) + \left\|\partial_t\left({}^{\nu,\theta}q^{WFT}(t)\right)\right\| \le \sum_j T.V.(\rho_{j,0}) + \sum_j |\mu_j - \mu_{j-1}|. \tag{29}$$

Since $\max_j v_j \Delta t_{j,\nu} = \Delta x_\nu = 2^{-\nu}\Delta x$, we get:

Theorem 3 *Assume that (H1), (H2), (21) hold true and that $\rho_{j,0}$ are of bounded variation. Then the following estimate holds true:*

$$\sup_{t\in[0,T]} \|(\zeta,\iota)(t)\|$$

$$\le \left(2^{-\nu}\Delta x\right)^2 \prod_{j=2}^{P} \max\left\{\frac{v_j}{v_{j-1}}, 1\right\} \left(\sum_j T.V.(\rho_{j,0}) + \sum_j |\mu_j - \mu_{j-1}|\right).$$

We are now ready to prove the following:

Proposition 2 *Assume that (H1), (H2), (21) hold true and that $\rho_{j,0}$ are of bounded variation. Let Y_i^{UE}, $i = 1, 2$, indicate the numerical approximation of Y_i via the Upwind-Euler steepest descent scheme of Section 4. Then there exists a constant K_1 depending only on the data of the problem:*

$$K_1 = K_1\left(\|\alpha_1\|_{L^1}, Lip(\alpha_2), \|\alpha_2\|_\infty, Lip(\psi), \|\psi\|_\infty, v_P, \mu_j, T.V.(\rho_{j,0})\right),$$

where $Lip(\cdot)$ indicates the Lipschitz constant of a function, $\|\cdot\|_\infty$ the L^∞ norm and $j = 1, \dots, P$, such that the following estimates hold:

$$\left\|Y_1^{WFT} - \pi_{PC}(Y_1^{UE})\right\| \le K_1 \sup_{t\in[0,T]} \|(\zeta,\iota)(t)\|,$$

where π_{PC} is the projection over piecewise constant functions as in (22) and

$$\|Y_2^{WFT} - Y_2^{UE}\| \le K_1 \sup_{t\in[0,T]} \|(\zeta,\iota)(t)\|.$$

Proof From (9) we have:

$$\left\|Y_1^{WFT} - \pi_{PC}(Y_1^{UE})\right\| \le \|\alpha_1\|_{L^1} \sup_{t\in[0,T]} \|(\zeta,\iota)(t)\|,$$

and

$$\|Y_2^{WFT} - Y_2^{UE}\| \le$$

$$\left(Lip(\alpha_2)\, v_P\left(\|\psi\|_\infty + 2\mu_P\right) \sup_{t\in[0,T]} \|{}^{\nu,\theta}(\xi,\eta)^{WFT}(t)\| \sup_{t\in[0,T]} T.V.({}^{\nu,\theta}\rho^{WFT}(t)) + \|\alpha_2\|_\infty\, v_P\, Lip(\psi) \sup_{t\in[0,T]} \|{}^{\nu,\theta}(\xi,\eta)^{WFT}(t)\| \sup_{t\in[0,T]} T.V.({}^{\nu,\theta}\rho^{WFT}(t))\right)$$

$$\cdot \sup_{t\in[0,T]} \|(\zeta,\iota)(t)\|.$$

By (28) and (29) we conclude.

We are now ready to state our main convergence result:

Theorem 4 *Assume that (H1), (H2), (21) hold true and that $\rho_{j,0}$ are of bounded variation. Fixing ν, if $\delta(u_{\nu,\theta}) = \bar{\delta}$, $h_\theta \geq \bar{h} > 0$, for all θ, and $\tau_k^{\nu,\theta} \to \bar{\tau}_k$ as $\theta \to +\infty$, then $u_{\nu,\theta}$ strongly converges in L^1 to some $\bar{u} \in \mathcal{U}_C$ as $\theta \to +\infty$ and*

$$\nabla_\xi J(\bar{u}) \leq K_2\, 2^{-\nu}\, \Delta x$$

where K_2 depends only on the data of the problem as for K_1 (of Proposition 2) and on v_j, $j = 1, \ldots, P$.

Proof Clearly $u_{\nu,\theta}$ strongly converges in L^1 to some $\bar{u}$, moreover by Helly theorem $\bar{u} \in \mathcal{U}_C$.
Now from Proposition 1, we have that $\nabla_\xi J(u_{\nu,\theta}) = Y_1^{WFT} + Y_2^{WFT}$. The tangent vectors ${}^{\nu,\theta}(\xi,\eta)^{WFT}$ converge as $\theta \to +\infty$, in the sense that the positions and values of shifts converge. Then we get that $\nabla_\xi J(u_{\nu,\theta})$ converges to $\nabla_\xi J(\bar{u})$.
Now since $\tau_k^{\nu,\theta} \to \bar{\tau}_k$ we have that Y_1^{UE} and Y_2^{UE} are bounded by $\Delta t_{1,\nu}$ (times a constant depending only on the data of the problem as for K_1). Thus we conclude by Theorem 3 and Proposition 2.

6 Simulations

In this Section we test the Euler-Upwind steepest descent algorithm on two test cases.

Consider first a supply chain characterized by 11 arcs with the following input function:

$$u(t) = \begin{cases} u_1 & 0 \leq t \leq \tau_1, \\ u_2 & \tau_1 < t \leq \tau_2, \\ u_3 & \tau_2 < t \leq T. \end{cases}$$

We assume that the supply chain is initially empty and set $v_j = 1\ \forall j = 1, ..., 11$ and

$$\mu_1 = 200,\ \mu_2 = 75,\ \mu_3 = 100,\ \mu_4 = 65,\ \mu_5 = 150,$$

$$\mu_6 = 75,\ \mu_7 = 30,\ \mu_8 = 100,\ \mu_9 = 80,\ \mu_{10} = 100,\ \mu_{11} = 120.$$

For simplicity we also set $\alpha_1 \equiv 1$ and $\alpha_2 \equiv 0$ and analyze two different cases:

Case a) $u_1 = 90, u_2 = 100, u_3 = 125, T = 10$, initial values $(\tau_1, \tau_2) = (1, 3)$;
Case b) $u_1 = 100, u_2 = 90, u_3 = 125, T = 10$, initial values $(\tau_1, \tau_2) = (4, 5)$.

As time and space grid meshes we choose $\Delta x = 0.02$ and $\Delta t = 0.016$ so as to satisfy the CFL condition. We use the condition that J remains unchanged for five runnings of the algorithm as forced stop criterion. The times τ_1 and τ_2 found by the algorithm are:

Case a) $\tau_1 \simeq 8.98$, $\tau_2 \simeq 9.14$: as expected both τ_1 and τ_2 run toward T; in fact, in order to minimize the queues, the optimization algorithm tends to reduce the inflow levels which increase the queues (i. e. u_2 and u_3).

Case b) $\tau_1 = 0$, $\tau_2 \simeq 9.05$: τ_1 runs to zero and τ_2 runs toward T; as in the previous case, the optimization algorithm works to reduce the inflow levels which lead to queues increasing (i. e. u_1 and u_3).

In Table 1 we report the numerical values of τ_1, τ_2 and J at each iteration of the steepest descent algorithm for Case a).

Table 1 Case *a*: J versus τ_1, τ_2 in 42 iterations of the steepest descent algorithm.

Iteration	τ_1	τ_2	J_1	Iteration	τ_1	τ_2	J_1
1	1	3	117799.059	22	8.873	9.076	69504.563
2	2.595	5.988	89474.759	23	8.887	9.084	69503.235
3	3.870	7.480	79616.859	24	8.897	9.093	69501.100
4	4.893	8.228	75291.519	25	8.906	9.099	69501.100
5	5.710	8.600	73053.659	26	8.915	9.105	69500.948
6	6.365	8.788	71737.0579	27	8.923	9.110	69500.948
7	6.888	8.880	70923.172	28	8.931	9.115	69500.073
8	7.306	8.926	70419.523	29	8.937	9.119	69500.073
9	7.640	8.957	70092.102	30	8.942	9.124	69500.061
10	7.907	8.977	69879.287	31	8.949	9.1276	69499.327
11	8.120	8.987	69749.807	32	8.954	9.130	69499.327
12	8.291	8.998	69660.449	33	8.959	9.134	69499.327
13	8.427	9.005	69608.289	34	8.964	9.137	69498.722
14	8.538	9.012	69570.370	35	8.968	9.139	69498.722
15	8.625	9.017	69544.690	36	8.972	9.140	69498.722
16	8.694	9.022	69530.770	37	8.976	8.972	69498.245
17	8.748	9.028	69521.531	38	8.978	9.144	69498.245
18	8.790	9.035	69514.2101	39	8.981	9.146	69498.245
19	8.818	9.047	69509.809	40	8.984	9.147	69498.245
20	8.839	9.058	69507.807	41	8.986	9.149	69498.245
21	8.858	9.066	69506.164	42	8.989	9.150	69498.245

Figure 2, respectively 3, depicts the values assumed by J, respectively (τ_1, τ_2), at each iteration step for Case a).

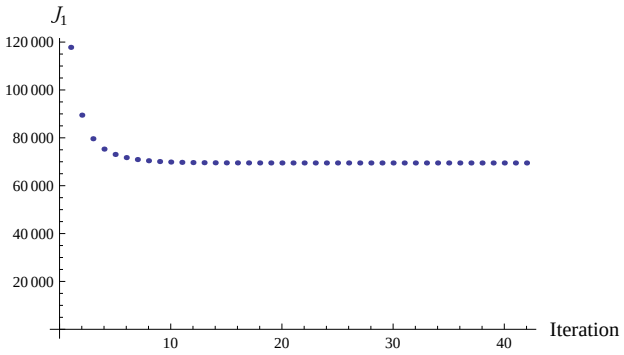


Fig. 2 Supply chain with 11 arcs, Case *a*. J versus iteration steps.

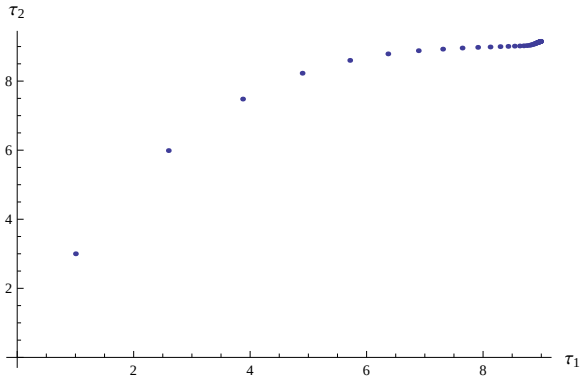


Fig. 3 Supply chain with 11 arcs, Case *a*. Path followed by the steepest descent algorithm in the plane (τ_1, τ_2).

The behaviour of the cost functional J in the plane (τ_1, τ_2), is reported for Case b) in Figure 4, to confirm the goodness of the steepest descent algorithm. Notice that since J decreases when the number of iteration increases, the updating of τ_1 and τ_2 values allows an effective decrement of queues at supply chain nodes.

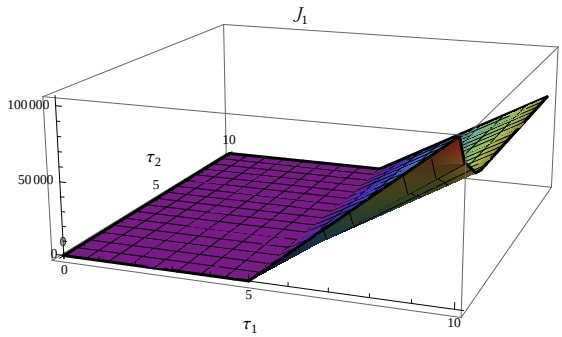


Fig. 4 Supply chain with 11 arcs, Case *b*. Behaviour of J_1 in the plane (τ_1, τ_2).

We now analyze now a supply chain with 2 arcs, maximal processing rates $\mu_1 = 200, \mu_2 = 75$ and lengths and processing rates of each processor equal to 1. We assume that processors and queues are empty at $t = 0$, i.e. $\rho_{j,0}(x) = 0$, $\forall\, x \in [0,1]$, $j = 1, 2$, $q_1(0) = 0$. The levels of the input flow are $u_1 = 100$, $u_2 = 80$, $u_3 = 50$. The total simulation time is $T = 20$ and numerical approximations are made with $\Delta x = 0.02, \Delta t = 0.016$. The aim is to optimize $J = J_1 + J_2$,with $\alpha_1 \equiv \alpha_2 \equiv 0.5$, i.e. minimize the queue handling a pre-assigned piecewise constant outflow:

$$\bar{\psi} = \psi(t) = \begin{cases} 100 & 0 \le t \le 10, \\ 75 & 10 < t \le T. \end{cases}$$

Figures 5 and 6 show the values assumed by J at each iteration step and the "path" followed by the steepest descent algorithm in the plane (τ_1, τ_2), starting with initial searching point $(\tau_1, \tau_2) = (5, 12)$. We observe that according to the aim of minimizing the queue, J is a decreasing function and, moreover, as expected the flux on the last arc is equal to the final outflow value. Finally J is minimized (its value is zero) by $(t_1, t_2) = (0, 0)$.

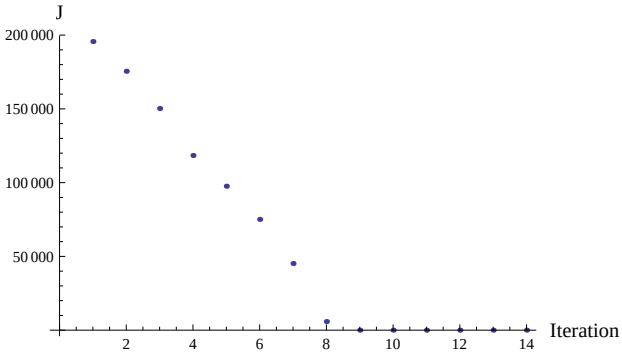


Fig. 5 Supply chain with 2 arcs: J versus iteration steps.

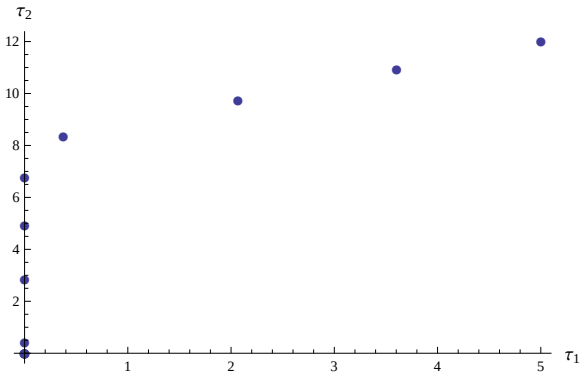


Fig. 6 Supply chain with 2 arcs: "path" followed by the steepest descent algorithm in the plane (τ_1, τ_2).

References

1. Armbruster, D., Degond, P., Ringhofer, C.: A model for the dynamics of large queueing networks and supply chains, SIAM Journal on Applied Mathematics, 66 (3), 896 - 920 (2006).
2. Armbruster, D., Degond, P., Ringhofer, C.: Kinetic and fluid models for supply chains supporting policy attributes, Transportation Theory Statist. Phys., 2006b (2006).
3. Armbruster, D., Marthaler, D., Ringhofer, C.: Kinetic and fluid model hierarchies for supply chains, SIAM J. on Multiscale Modeling, 2 (1), 43 - 61 (2004).
4. Bonnans, J.F., Gilbert, J.C., Lemaréchal, C., Sagastizàbal, C.A.: Numerical Optimization: Theoretical and Practical Aspects, 419 pages. Springer, New York (2003).
5. Bressan, A.: A variational calculus for discontinuous solutions of systems of conservation laws, Communications on PDE, 20 (9), 1491 - 1552 (1995).
6. Bressan, A.: Hyperbolic Systems of Conservation Laws - The One-dimensional Cauchy Problem, 250 pages. Oxford Univ. Press (2000).
7. Bressan, A., Crasta, G., Piccoli, B.: Well-Posedness of the Cauchy Problem for $n \times n$ Systems of Conservation Laws, Memoirs of the American Mathematical Society, vol. 146, n. 694 (2000).
8. Bretti, G., D'Apice, C., Manzo, R., Piccoli, B.: A continuum-discrete model for supply chains dynamics, Netw. Heterog. Media, 2 (4), 661 - 694 (2007).
9. Cutolo, A., Piccoli, B., Rarità, L.: An Upwind-Euler scheme for an ODE-PDE model of supply chains, Siam Journal on Scientific Computing, 33(4), 1669 - 1688 (2011).
10. D'Apice, C., Goettlich, S., Herty, M., Piccoli, B.: Modeling, Simulation and Optimization of Supply Chains, 216 pages. SIAM, Philadelphia PA, USA, 2010.
11. D'Apice, C., Manzo, R.: A fluid dynamic model for supply chains, Netw. Heterog. Media, 1 (3), 379 - 398 (2006).
12. C. D'Apice, R. Manzo, B. Piccoli: Modelling supply networks with partial differential equations, Quarterly of Applied Mathematics, 67(3), 419 - 440 (2009).
13. D'Apice, C., Manzo, R., Piccoli, B.: Optimal input flows for a PDE-ODE model of supply chains, to appear on Communication in Mathematical Sciences;
14. Forrester, J.W.: Industrial dynamics, 464 pages. MIT Press, Cambridge, MA (1964).
15. Garavello, M., Piccoli, B.: Traffic flows on networks, 243 pages. American Institute of Mathematical Sciences, Springfield, MO (2006).
16. Göttlich, S., Herty, M., Klar, A.: Network models for supply chains, Communication in Mathematical Sciences, 3(4), 545 - 559 (2005).
17. Göttlich, S., Herty, M., Klar, A.: Modelling and Optimization of Supply Chains on Complex Networks, Communication in Mathematical Sciences, 4(2), 315 - 330 (2006).
18. Göttlich, S., Herty, M., Ringhofer, C.: Optimization of order policies in supply networks, European J. Oper. Res. 202(2), 456 - 465 (2010).
19. Herty, M., Klar, A.: Modeling, Simulation, and Optimization of Traffic Flow Networks, SIAM J. Sci. Comput., 25(3), 1066 - 1087 (2003).
20. Herty, M., Klar, A., Piccoli, B.: Existence of solutions for supply chain models based on partial differential equations, SIAM J. Math. An., 39(1), 160 - 173 (2007).
21. Helbin,g D. , Lämmer, S., Seidel, T., Seba, P., Platkowski, T.: Physics, stability and dynamics of supply networks, Physical Review E 70, 066116 (2004).
22. Helbing, D., Lämmer, S.: Supply and production networks: from the bullwhip effect to business cycles, in: D. Armbruster, A. S. Mikhailov, and K. Kaneko (eds.), Networks of Interacting Machines: Production Organization in Complex Industrial Systems and Biological Cells, World Scientific, Singapore, 33 - 66 (2005).
23. Kirchner, C., Herty, M., Göttlich, S. and Klar, A.: Optimal control for continuous supply network models, Netw. Heterog. Media, 1(4), 675 - 688 (2006).
24. Leveque, R.J.: Finite Volume Methods for Hyperbolic Problems, 578 pages. Cambridge University Press (2002).